A simple alternative for accurate finite-element modeling in curved domains

V. Ruas [a, b]

a. ∂'Alembert, Sorbonne Universités, Université Pierre et Marie Curie, Paris 6, UMR 7190
b. Institut Jean Le Rond d'Alembert, CNRS, UMR 7190, Paris, France

Résumé :

Une des raisons de l'indéniable succès de la méthode des éléments finis dans les applications industrielles est sa grande versatilité pour la simulation numérique dans des domaines courbes. Dans ce cas la technique isoparamétrique sur des maillages constitués de triangles ou tetraèdres courbes a été introduite il y a longtemps, afin de préserver la capacité d'approximation optimale qui s'applique au cas de maillages en éléments droits de domaines polygonaux ou polyédriques. Cependant, outre des complications géométriques, cette technique exige la manipulation de fonctions rationnelles, ce qui oblige l'utilisateur à effectuer des choix d'intégration numérique parfois délicats. On présente une alternative simple pour traiter des conditions aux limites de Dirichlet, évitant tous ces inconvénients, sans érosion de la qualité des résultats. Il s'agit d'une approche qui dispense les éléments courbes, basée uniquement sur la algèbre polynomiale, étant ainsi bien adaptée à un code industriel. Son universalité est illustrée au travers d'exemples sur écoulements visqueux et en élasticité linéaire..

Abstract :

One of the reasons for the great success of the finite element method in industry is its versatility to deal with problems posed in curved domains. In this case method's isoparametric version for meshes consisting of curved triangles or tetrahedra has been mostly employed to recover the optimal approximation properties known to hold for standard elements in the case of polytopic domains. However, besides geometric inconveniences, the isoparametric technique helplessly requires the manipulation of rational functions and the use of numerical integration. We consider a simple alternative to deal with Dirichlet boundary conditions that bypasses these drawbacks, without eroding qualitative approximation properties. Our technique is based only on polynomial algebra in N-simplex and can do without curved elements. Its universality for use in industrial codes is illustrated in the framework of both incompressible viscous flow and small deformations of elastic solids.

Mots clefs : bord courbe – code industriel – éléments finis – fonction de forme polynomiale – ordre optimal.

Key-words : curved boundary – finite elements – industrial code – optimal order – polynomial shape function.

1 Introduction

This work deals with a finite element method for solving boundary value problem posed in a two- or three-dimensional domain, with a smooth curved boundary of arbitrary shape. The principle it is based upon is close to the technique called interpolated Dirichlet boundary conditions studied in [2] for two-dimensional problems. Although the latter technique is very intuitive and is known since the seventies (cf. [5} and [10]), it has been of limited use so far. Among the reasons for this we could quote its difficult implementation, the lack of an extension to three-dimensional problems, and most of all, restrictions on the choice of boundary nodal points to reach optimal convergence rates. In contrast our method is simple to implement in both two- and three-dimensional geometries. Moreover optimality is attained very naturally in both cases for various choices of boundary nodal points.

Without loss of essential aspects, our methodology can be perfectly described taking as a model simple linear partial differential equations with Dirichlet boundary conditions. We consider for example the Poisson equation solved by different *N*-simplex based methods, incorporating degrees of freedom other than function values at the mesh vertices. If standard quadratic Lagrange finite elements are employed, it is well-known that approximations of an order not greater than 1.5 in the energy norm are generated (cf. [3]), in contrast to the second order ones that apply to the case of a polygonal or polyhedral domain, assuming that the solution is sufficiently smooth. If we are to recover the optimal second order approximation property, something different has to be done. Since long the isoparametric version of the finite element method for meshes consisting of curved triangles or tetrahedra (cf. [11]), has been considered as the ideal way to achieve this. It turns out that, besides a more elaborated description of the mesh, the isoparametric technique inevitably leads to the integration of rational functions to compute the system matrix, which raises the delicate question on how to choose the right numerical quadrature formula in the master element.

In contrast, in the technique to be considered in this paper exact integration can always be used for this purpose, since we only have to deal with polynomial integrands. Moreover the element geometry remains the same as in the case of polygonal or polyhedral domains. It is noteworthy that both advantages are conjugated with the fact that no erosion of qualitative approximation properties results from the application of our technique, as compared to the equivalent isoparametric one.

We should also emphasize that this approach is particularly handy, whenever the finite element method under consideration has normal components or normal derivatives as degrees of freedom. Indeed in this case the definition of isoparametric finite element analogs is not always so clear or straightforward (see e.g. [1]).

An outline of the paper is as follows. In Section 2 we describe our method to solve a model Poisson problem with Dirichlet boundary conditions in a smooth curved two-dimensional domain with conforming Lagrange finite elements based on meshes with straight triangles, in connection with a standard Galerkin formulation. We recall the error estimates established in [7] for this method. In Section 3 we assess its approximation properties, by solving problems posed in a curved two-dimensional domain with piecewise quadratic functions. More specifically circular membrane problems are solved, and we use our methodology to represent the velocity in a circular Couette flow. Numerical experiments are further carried out in Section 4, again in the framework of curved membranes, but also for small plane deformations of plates. However in contrast to Section 3 here the simulations are done with an adaptation of our technique to a Hermite analog (cf. [8]) of the Raviart-Thomas mixed finite element of the lowest order [6]. We conclude in Section 5 with a few comments.

2 Method description

As a model we consider the Poisson equation with Dirichlet boundary conditions in an *N*-dimensional smooth domain Ω with boundary $\partial\Omega$ for *N*=2 or *N*=3, that is, $-\Delta u = f$ in Ω, $u = d$ on $\partial\Omega$, where *f* and *d* are given functions defined in Ω and on $\partial\Omega$, having suitable regularity properties. We shall be

dealing with approximations of *u* of order *k* for *k* > 1 in the standard energy norm, assuming that *f, d* and Ω are sufficiently smooth.

Although the method to be described below applies to any spatial dimension, for the sake of simplicity we confine its description to the two-dimensional case.

Let us then be given a partition $\mathbf{T}_h$ of Ω into straight triangles satisfying the usual compatibility conditions (see [3]). $\mathbf{T}_h$ is assumed to belong to a uniformly regular family of partitions. Let Ω_h be the polygonal domain formed by the union of the triangles in $\mathbf{T}_h$ and $\partial\Omega_h$ be its boundary. Further h_T being the diameter of a triangle *T* in $\mathbf{T}_h$, as usual we denote by *h* the maximum of the h_T s as *T* sweeps $\mathbf{T}_h$. Notice that if Ω is convex Ω_h is a proper subset thereof. We make the more than reasonable assumptions on the mesh that no element in $\mathbf{T}_h$ has more than one edge on $\partial\Omega_h$.

We also need some definitions regarding the skin comprised between $\partial\Omega_h$ and $\partial\Omega$. First of all, in order to avoid non essential technicalities, we assume that the mesh is constructed in such a way that convex and concave portions of $\partial\Omega$ correspond to convex and concave portions of $\partial\Omega_h$. This property is guaranteed if the points separating such portions of $\partial\Omega$ are vertices of polygon Ω_h. In doing so, let $\mathbf{S}_h$ be the subset of $\mathbf{T}_h$ consisting of triangles having one edge on $\partial\Omega_h$. Now for every triangle *T* belonging to $\mathbf{S}_h$ we denote by Δ_T the skin portion delimited by $\partial\Omega$ and the edge e_T of *T* whose end-points belong to $\partial\Omega$ and let *T* ' be the union of *T* and Δ_T (see Figure 1).
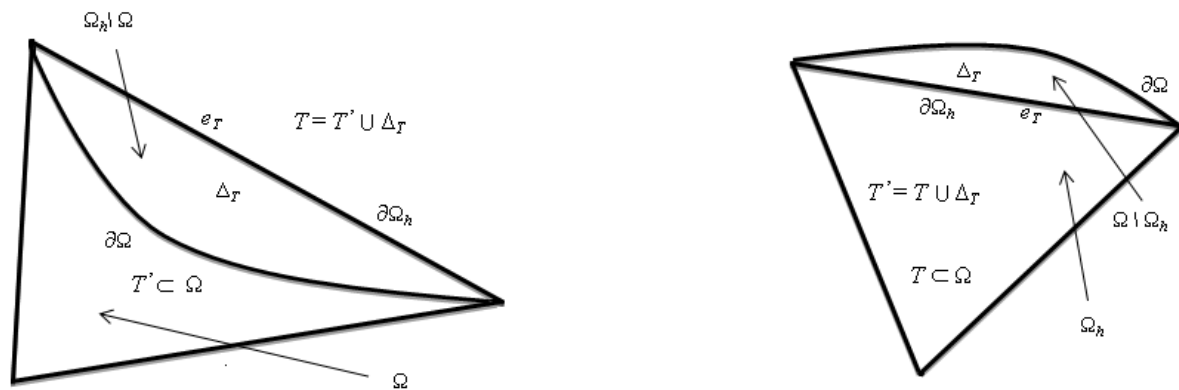
Skin portion Δ_T for a triangle *T* next to a convex (right) or a concave (left) portion of $\partial\Omega$
Figure 1

Next we introduce two sets of functions V_h and W_h associated with $\mathbf{T}_h$. V_h is the standard Lagrange finite element space consisting of continuous functions *v* defined in Ω_h that vanish on $\partial\Omega_h$, whose restriction to every triangle *T* in $\mathbf{T}_h$ is a polynomial of degree less than or equal to *k* for *k* > *1*. For convenience we extend by zero every function *v* in V_h to $\Omega \setminus \Omega_h$.

W_h in turn is the set of functions defined in Ω_h having the properties listed below

1. The restriction of *w* in W_h to every *T* in $\mathbf{T}_h$ is a polynomial of degree less than or equal to *k* ;

2. Every *w* in W_h is continuous in Ω_h and $w(S) = d(S)$ for every mesh vertex *S* located on $\partial\Omega_h$;

3. A function *w* in W_h is also defined in $\Omega \setminus \Omega_h$, in such a way that its polynomial expression in a triangle *T* belonging to $\mathbf{S}_h$ also applies to points in the skin portion Δ_T ;

4. For all *T* belonging to $\mathbf{S}_h$, $w(P) = d(P)$ at every point *P* of $\partial\Omega$ located on the lines passing through the vertex O_T of *T* not belonging to $\partial\Omega$ and the *k*–1 points *M* of e_T different from a vertex of *T* lying among those that subdivide this edge into *k* segments of equal length (cf. Figure 2).
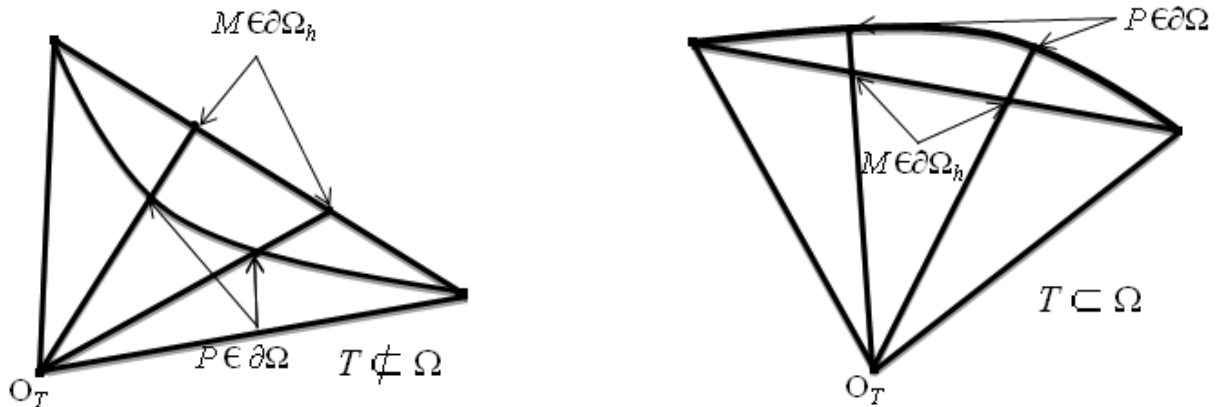
Construction of nodes *P* on ∂Ω for set W_h related to lagrangian nodes *M* on ∂Ω$_h$ for *k = 3*
Figure 2

<u>Remark:</u> The construction of the nodes associated with W_h located on ∂Ω$_h$ advocated in item 4 is not mandatory. Notice that it differs from the intuitive construction of such nodes lying on normals to edges of ∂Ω$_h$ commonly used in the isoparametric technique. The main advantage of this proposal is an easy determination of boundary node coordinates by linearity, using a supposedly available analytical expression of ∂Ω. Actually the choice of boundary nodes ensuring our method's optimality is really wide, in contrast to the restrictions inherent to the interpolated boundary condition method (cf. [2]). ∎

The fact that W_h is a non empty finite-dimensional manifold was established in [7].

Next we set the problem associated with the sets of functions V_h and W_h, whose solution is an approximation u_h of the solution *u* to the Poisson equation. Taking any regular extension of *f* to Ω$_h$ \ Ω and still denoting the resulting function by *f*, u_h is determined as the solution of the following variational problem:

$$u_h \text{ lies in } W_h \text{ and fulfills } \int_{\Omega_h} grad \; u_h \cdot grad \; v \; d\text{x} = \int_{\Omega_h} f \, v \; d\text{x} \quad \text{for all } v \text{ in } V_h . \tag{1}$$

According to [7], provided *h* is sufficiently small, problem (1) has a unique solution. Moreover the underlying bilinear form is uniformly stable on $W_h \times V_h$ in the sense of Babuska-Brezzi (cf. [7]). This leads to the conclusion that the approximation method associated with (1) is a *k*-th order method in the natural energy norm, as long as *u* is sufficiently smooth and all the $\mathbf{T}_h$ s under consideration belong to a regular family of partitions of Ω in the sense of [3]. In short $[\int_{\Omega_h} / \; grad \; (u_h - u) \; |^2 \; d\text{x}]^{1/2}$ is an O(h^k), under such assumptions.

3 Numerical experiments with quadratic elements

In order to show the effectiveness of the technique studied in this work to take into account Dirichlet boundary conditions prescribed on curved boundaries, we report in this section significant numerical results for some academic test-problems with known exact solution, taking *k*=2. We selected two classical applications in Continuum Mechanics, namely the deflexion undergone by a plane membrane under the action of forces orthogonal to its plane, and the laminar flow of an incompressible viscous fluid between two rotating cylinders.

3.1 Deflexions of an elastic membrane

In the small strain regime a homogeneous elastic membrane whose edge is kept fixed, subjected to a load distribution *g* applied perpendicularly to its plane, Π is governed by the Poisson equation with homogeneous Dirichlet boundary conditions. More specifically, in appropriate dimensionless form the deflexion *u* in the direction orthogonal to Π satisfies $-\Delta u = f$ in the domain Ω occupied by the membrane in Π, where *f = c g* for a suitable constant *c*. For the sake of simplicity we consider that Ω is the unit disk with center at the origin O of a cartesian coordinate system (O,*x*,*y*) attached to Π. Taking *g* of the conical form *αr* where $r = (x^2 + y^2)^{1/2}$ the exact solution is given by $u(x,y) = α (1 − r^3)$ / 9c. In our computations we took *α = 9c*, and used meshes successively refined consisting of $2M^2$ triangles for $M=2^m$ with *m* = 2, 3, 4, 5, 6. For better visibility quite abusively we set *h = 1/M* . The resulting errors in the following senses are displayed in Table 1. In the third row we show the errors in the energy norm. In the fourth row the mean square norms of ($u − u_h$) in $Ω_h$ are given, while in the last row the maximum absolute errors at the mesh nodes are supplied. In order to make sure that there was no favorable effect owing to the particular form of the domain and/or the exact solution, we also computed with the same meshes using the traditional approach. This consists of prescribing zero boundary values at the mid-points of the edges e_T, besides the vertices of $\partial Ω_h$. Corresponding errors are supplied in Table 2. Observation of both tables confirm second order convergence in the energy norm, while the traditional approach yields only $O(h^{3/2})$ approximations in the same sense, as predicted in classical books (cf. [3]). Even better news come from the errors in the mean-square sense. We observe third order convergence for our method, in contrast to the second order convergence of the traditional approach. As for the maximum errors at the nodes, both approaches seem to be equivalent.

Table 1 – Errors for the membrane problem solved with the new method for *k*=2

M →	4	8	16	32	64
h →	0.250000	0.125000	0.062500	0.031250	0.015625
Energy norm of $u_h − u$	0.14007 x 10^{-1}	0.36168 x 10^{-2}	0.91850 x 10^{-3}	0.23151 x 10^{-3}	0.58128 x 10^{-4}
Mean-square norm of $u_h − u$	0.43895 x 10^{-3}	0.56460 x 10^{-4}	0.71709 x 10^{-5}	0.90592 x 10^{-6}	0.12428 x 10^{-6}
Max. $|u_h−u|$ at mesh nodes	0.14376 x 10^{-1}	0.36093 x 10^{-2}	0.90327 x 10^{-3}	0.22588 x 10^{-3}	0.56473 x 10^{-4}

Table 2 – Errors for the membrane problem solved with the classical approach for *k*=2

M →	4	8	16	32	64
h →	0.250000	0.125000	0.062500	0.031250	0.015625
Energy norm of $u_h − u$	0.54344 x 10^{-1}	0.19690 x 10^{-1}	0.70417 x 10^{-2}	0.25026 x 10^{-2}	0.88700 x 10^{-3}
Mean-square norm of $u_h − u$	0.81891 x 10^{-2}	0.19879 x 10^{-2}	0.48790 x 10^{-3}	0.12070 x 10^{-3}	0.29979 x 10^{-4}
Max $|u_h−u|$ at the mesh nodes	0.14376 x 10^{-1}	0.36093 x 10^{-2}	0.90327 x 10^{-3}	0.22588 x 10^{-3}	0.56473 x 10^{-4}

3.2 Couette flow between rotating cylinders

The aim of the experiments reported in this sub-section is to assess the behavior of our method in the case where Ω is not convex. More specifically Ω is the annulus delimited by the circles given by $r = r_e$ $r = r_i$ with $r^2 = x^2 + y^2$, with $r_i < r_e$. This annulus represents the cross section of the domain comprised between two concentric cylinders with radii r_e and r_i, filled with a viscous incompressible flow with viscosity μ and density ρ. The inner cylinder rotates with angular velocity ω_i and the outer cylinder is kept fixed. We assume flow conditions under which the flow is laminar. In this case the velocity field $\mathbf{v} = (v_x, v_y, v_z)$ referred to a cartesian frame (O, x, y, z) such that the z-axis coincides with the axis of both cylinders is given by $v_x(x, y) = - y\, \omega(r)$ and $v_y(x, y) = - v_x(y, x)$, where $\omega(r)$ is the angular velocity of the fluid at a distance from the z-axis equal to r. It is well-known that $\omega(r) = \omega_i (r_i/r)^2 (r_e^2 - r^2) / (r_e^2 - r_i^2)$. The hydrostatic pressure p in the fluid in turn depends only on r and is given by $dp/dr = \rho\, r\, \omega^2(r)$. Of course, since the exact solution is known, it is no point attempting to simulate this kind of flow. Instead our experiments consist of approximating by piecewise quadratic finite elements the velocity components v_x and v_y and field $\mathbf{v}$, which together with p satisfy the momentum equation in Ω, namely

$$- \mu\, \Delta v_x + \mathbf{v} \cdot grad\, v_x = - x\, \rho\, \omega^2(r) \text{ and } - \mu\, \Delta v_y + \mathbf{v} \cdot grad\, v_y = - y\, \rho\, \omega^2(r)$$

with the Dirichlet boundary conditions $v_x(x, y) = - y\omega_i$ and $v_y(x, y) = x\omega_i$ if $r = r_i$ and $v_x = v_y = 0$ if $r = r_e$. In short, letting d be the function defined on $\partial\Omega$ in accordance with the above boundary data, and setting $f(x, y) = - x\, \rho\, \omega^2(r)$ (resp. $f(x, y) = y\, \rho\, \omega^2(r)$), we approximate v_x (resp. v_y) by u_h in W_h for $k=2$, as the solution of the following convection-diffusion equation in varirational form:

$$\int_{\Omega^h} [\mu\, grad\, u_h \cdot grad\, v + \mathbf{v} \cdot grad\, u_h\, v]\, d\mathrm{x} = \int_{\Omega^h} f v\, d\mathrm{x} \quad \text{for all } v \text{ in } V_h . \tag{2}$$

In order to take advantage of symmetry we solve (2) in the half annulus corresponding to $x > 0$ (resp. $y > 0$), by prescribing homogeneous Neumann boundary conditions at $x=0$ (resp. $y=0$). We take $\omega_i =1$, and $r_e = 1$, $r_i = 1/2$. The meshes of this computational domain consist of $8M^2$ triangles constructed by subdividing the range of the radial coordinate r into M equal segments, and its total aperture equal to π into $4M$ equal angles (with $M > 1$). Setting for convenience $h = \pi / 4M$ and $u = v_x$, we give in Table 3 the errors $u - u_h$ measured in the energy norm, for $M = 2, 4, 8, 16, 32$. Akin to Table 1, we supply again the mean square norm of the errors, together with the maximum absolute values of $u - u_h$ at the mesh nodes. As one can observe, in this case too the numerical results confirm that our method is of order two in the energy norm and of order three in the mean square sense. However in this example a super-convergence effect occurs, for the maximum errors at the nodes decrease almost as an $O(h^4)$.

Table 3 – Errors for the Couette flow velocity component $u=v_x$ obtained with the new method for $k=2$

$4M \rightarrow$	8	16	32	64	128
$h \rightarrow$	0.392700	0.196350	0.098175	0.049087	0.024544
Energy norm of $u_h - u$	0.10690×10^{-0}	0.27930×10^{-1}	0.70862×10^{-2}	0.17789×10^{-2}	0.44522×10^{-3}
Mean-square norm of $u_h - u$	0.30589×10^{-2}	0.39321×10^{-3}	0.49837×10^{-4}	0.62551×10^{-5}	0.78301×10^{-6}
Max $|u_h - u|$ at the mesh nodes	0.22258×10^{-2}	0.20322×10^{-3}	0.15176×10^{-4}	0.10267×10^{-5}	0.66015×10^{-7}

4 Simulations using Hermite interpolation

In this section we apply the principles described in Section 2 to a finite element method based on Hermite interpolation, to show that the methodology employed in this work is as universal as can be. More specifically, we solve a few model problems of linear elasticity using a variant of the classical Raviart-Thomas mixed finite element of the lowest order [6], commonly known as RT_0. This variant studied in author's work [8] and [9] among other papers of his, is to be employed in the framework of variational formulations mimicking corresponding mixed formulations. A Hermite interpolation with discontinuous piecewise incomplete quadratic functions allows for better accuracy of an approximate unknown field in the mean square sense, as compared to the RT_0 finite element, though at equivalent cost. Unknown field's gradients in turn, such as deformations, are identically represented.

We solve two types of model problems posed in smooth curved two-dimensional domains. In Subsection 4.1 we consider again the membrane problem recast in mixed form, in which prescribed zero normal forces are treated as Dirichlet boundary conditions, while prescribed deflexions are regarded as Neumann boundary conditions. In Sub-section 4.2 we use the same numerical ingredients to determine the displacement field of a plate of curved shape in the small plane deformation regime, with prescribed normal forces on the outer edge of its mid-plane.

4.1 A stress-deflexion formulation for elastic membranes

We consider that the deflexion of a plane elastic membrane vanishes only on a part of its edge. On the complementary part we assume a zero normal force condition, that is, $\partial u/\partial n = 0$, where $\partial u(\cdot) /\partial n$ denotes the outer normal derivative along $\partial\Omega$. For the sake of simplicity we assume that the mesh $\mathbf{T}_h$ matches the transition points between both parts of $\partial\Omega$, in the sense that they are vertices of the corresponding partition of Ω into triangles.

In order to prescribe normal forces on the edge of the membrane, following [8], first we recast the membrane finite-element model (1) in a non standard variational form, namely:

$$ - \textstyle\sum_{T \text{ in } \mathbf{T}_h} \left[\; \int_T \; (\; \Delta u_h \, v + grad \, u_h \cdot grad \, v + u_h \Delta \, v \;) \; d\mathrm{x} \; \right] = \int_{\Omega_h} f \, v \, d\mathrm{x} \;\; \text{for all } v \text{ in } V_h \,, \tag{3} $$

where u_h the approximation of u in a set of functions U_h to be specified hereafter, and V_h is a set of (discontinuous) functions of the form $a \, \mathbf{x}^2 / 2 + \mathbf{b} \cdot \mathbf{x} + e$ in each triangle T of $\mathbf{T}_h$, a and e being real coefficients and $\mathbf{b}$ being a vector of $\mathbf{R}^2$. Then, like the flux variable in the RT_0 method, the gradient of v in V_h is of the form $a \, \mathbf{x} + \mathbf{b}$ and its normal component along an edge is constant according to [6]. We require that this normal component of every v in V_h along a mesh edge be single valued if the edge is common to two mesh triangles, or to vanish if the edge is contained in $\partial\Omega_h$ and corresponds to a zero normal force boundary condition. Actually the degrees of freedom of V_h are precisely these normal derivatives along the edges, besides the function mean values in the mesh elements (cf. [8]). Owing to this choice of degrees of freedom the local construction of functions in V_h must rely upon Hermite interpolation. Since this method represents the gradient of the unknown field in the same way as the RT_0 mixed method, both methods differ only in the (discontinuous) representation of the deflexion itself. Indeed in each triangle it is a linear function enriched with a quadratic term in the case of the Hermite method, whereas it is just constant for the mixed method. As long as Ω is a polygon, we can take $U_h = V_h$, for such a distinction renders the above described Hermite variant of RT_0 a second order method in the mean square sense (cf. [8]), in contrast to the mixed method, which is just of the first order in the same sense. Here we attempt to show that, unless a suitable U_h different from V_h is chosen, such a property no longer holds, in case Ω is a curved domain.

Our choice of U_h is a space defined in the same way as V_h, except for the mesh triangles T in the subset of $\mathbf{S}_h$ of those triangles having an edge upon which a zero normal derivative condition must be

enforced. However instead of enforcing this condition along such an edge, we require that the (constant) first order derivative of a function in U_h in the direction normal to it vanish along the tangent to the boundary at the intersection with it, of the line joining the mid-point of this edge to the opposite vertex. This means that for each boundary triangle we pick up the normal derivative boundary condition where it is prescribed, i.e., on the neighboring portion of the true boundary. This is exactly the counterpart for the Hermite finite element under study, of the technique designed to treat Dirichlet boundary conditions with Lagrange finite elements described in Section 2.

Unlike the experiments reported so far, in this sub-section we solve test-problems whose exact solution is not known. One of the aspects to be focused here is the response of our method in case of boundary concavities. Due to the impossibility to infer convergence rates on the basis of true error functions, we will attempt to understand method's behavior by observing the evolution of a certain quantity related to the numerical solution as the meshes are refined. Here a choice better than the mean-square norm is the maximum value at the element centroids. This is because the corresponding value of the exact solution lies necessarily in Ω_h, and hence the O(h) mean-square norm of the solution in the skin $\Omega \setminus \Omega_h$ will not dominate the order evaluation, should such a norm be employed.

Two test-problems were solved for rosette-shaped membranes illustrated in Figure 4. Before presenting corresponding results we first report those for a toy-problem in an ellipse with semi-axes 0.5 and 1.0, prescribing zero normal derivative along its boundary, whose exact solution is a polynomial of degree four. For such a problem the evolution as the mesh is refined of numerical solution's maximum absolute value at the centroids of the mesh elements was checked. This allowed to assess its convergence rates to the corresponding value of the exact solution for three different approaches, namely, the classical RT_0 method, its Hermite variant taking $U_h = V_h$ and the latter combined with our new method to approximate Dirichlet boundary conditions on curved boundaries. Here again the meshes employed in these computations are indexed by an integer M (setting $h=1/M$), and are constructed quite in the same way as in Sub-section 3.1 for a disk. From the error evolution measured in the mean-square norm, it turned out that the corresponding observed convergence rates are roughly 1, 5/3 and 2, respectively. This clearly indicates that the modification in order to take into account the normal derivative boundary condition by the Hermite variant of RT_0 is indeed necessary, if we wish to recover method's second order in the mean-square norm, known to hold for polygonal domains (cf. [8]). On the other hand a convergence rate of 2 is observed for the three methods as far as solution's maximum absolute value at element centroids is concerned, as one can infer from Table 4. Nevertheless, it is noteworthy that the accuracy of the boundary-modified Hermite variant of RT_0 in this respect is considerably improved, even for coarser meshes. This can also be observed in Table 4, taking into account that the maximum absolute value of the exact solution is 1.56250, up to the fifth decimal.
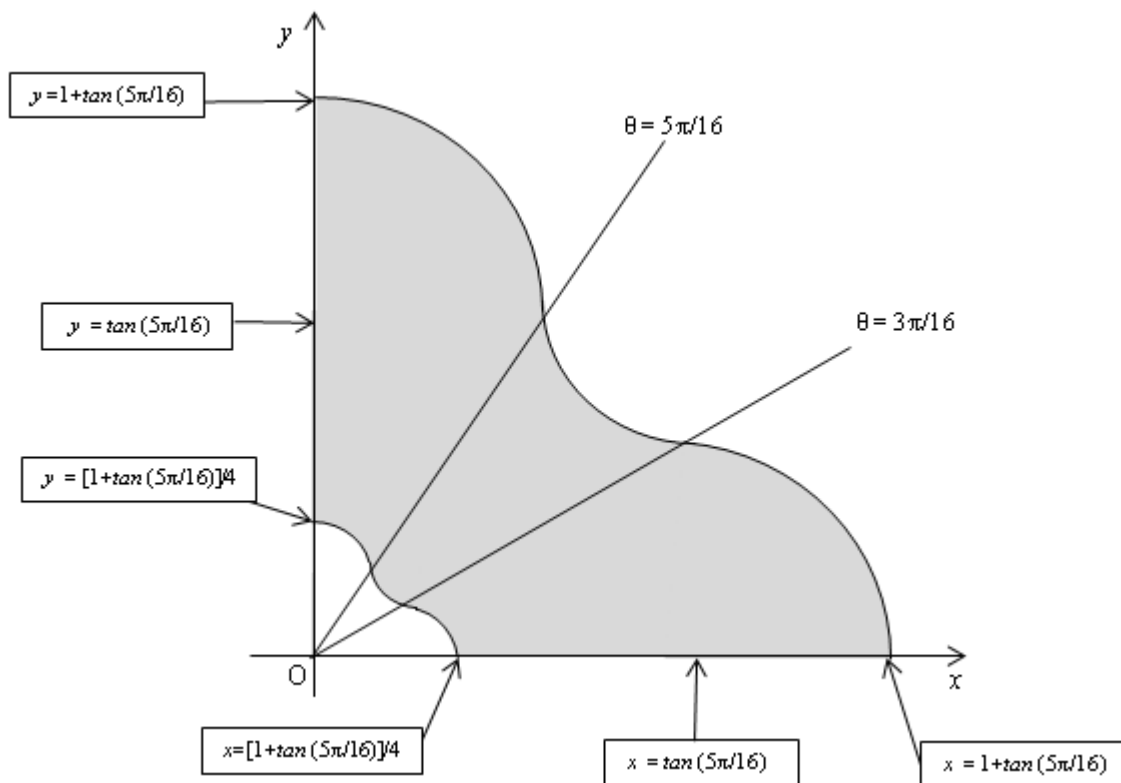
Table 4 – Maximum absolute value at element centroids of the solution to a toy-problem in an ellipse

$M \rightarrow$	8	16	32	64	128
$h \rightarrow$	0.01250000	0.00625000	0.00312500	0.00156250	0.00078125
Classical RT_0 mixed method	1.509333×10^{-2}	1.546930×10^{-2}	1.558024×10^{-2}	1.561229×10^{-2}	1.562206×10^{-2}
Hermite variant of RT_0 ($U_h = V_h$)	1.532269×10^{-2}	1.553026×10^{-2}	1.559596×10^{-2}	1.561629×10^{-2}	1.562283×10^{-2}
Modified Hermite variant of RT_0	1.556403×10^{-2}	1.561907×10^{-2}	1.562463×10^{-2}	1.562495×10^{-2}	1.562503×10^{-2}

Test-problem 4.1.1 – The membrane is symmetric with respect to both cartesian coordinate axes. It has a hole whose edge is a homothetical transformation of membrane's outer edge with center at the origin of the coordinate system and ratio equal to 1/4. Both its outer edge and inner edge consist of an assembly of quarter circles alternating a radius equal to 1 and $\beta = [tan(5\pi/16) -1] \approx 0.49660576$ for the outer edge, in such a way that they have the same tangent at common points. A quarter domain is of the form depicted in Figure 3. We assume that the deflexion vanishes on the edge of the hole, while on the outer edge of the membrane no normal forces act. We take a right hand side function $f \equiv 1$. Naturally enough, only a quarter domain is taken into account in the computations. Like in the previous test-problems a regular family of meshes indexed by an integer parameter M is employed. M being a multiple of 4, we construct $3M/4$ homothetical transformations Ω_l of Ω with center at the origin and ratio l/M, for $l = M/4, M/4+1, \ldots M-1$. θ being the polar angle, the sector given by $0 \le \theta \le \pi/2$ within Ω_l is subdivided into $2l$ equal sectors. The mesh vertices are the intersections with the boundary of Ω_l of the lines given by $\theta = m\pi/(2l)$, for $m=0, 1,\ldots, 2l$, resulting from such subdivisions into $2l$ equal angles. The total number of vertices equals $(M+1)^2 - (M/4)^2$, while the total number of elements generated by this procedure is $2[M^2 - (M/4)^2]$.

On the left part of Figure 4 an illustration of the whole domain is given, the hole being painted in black in order to represent a zero deflexion along its inner edge.

For simplicity we set $h = 2.5/M \approx (2+\beta)/M$ and solve the problem for $M=8,16,32,64$ and 128. Resulting numerical values supplied in Table 5 are the maximum absolute values at mesh triangle centroids of the solutions obtained by the classical approach, that is, taking $U_h = V_h$, and by the modification using the above defined space U_h. It is a little disappointing to figure out that, in contrast to the toy-problem in an ellipse, both methods behave rather identically for this test-problem with a presumably smooth exact solution. This could be due to the fact that here the domain has several boundary concavities, but anyway such an issue deserves further investigation.

A quarter rosette-shaped membrane with a hole supported on its inner edge

Figure 3
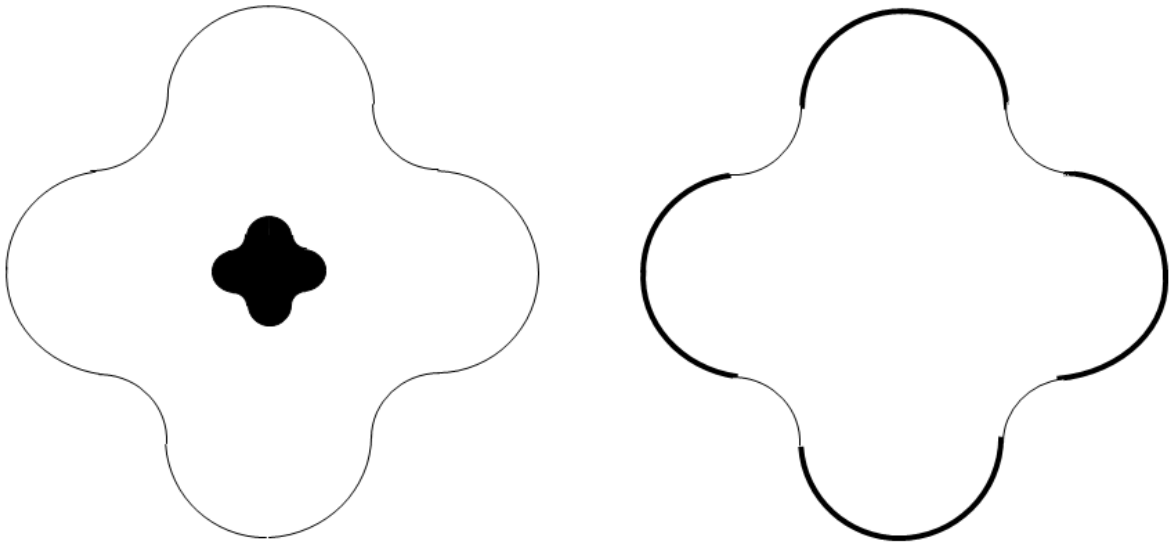
Geometry and boundary conditions for Test-problem 4.1.1 (left) and Test-problem 4.1.2 (right)
Figure 4

Table 5 – Solutions' maximum absolute values at element centroids for Test-problem 4.1.1

M →	8	16	32	64	128
h →	0.31250000	0.15625000	0.07812500	0.03906250	0.01953125
Hermite variant of RT_0 ($U_h=V_h$)	2.4089238	2.3097770	2.2735438	2.2623647	2.2610764
Modified Hermite variant of RT_0	2.4132353	2.3102900	2.7298998	2.2636612	2.2610798

Test-problem 4.1.2 – Here the membrane is of the form depicted on the right side of Figure 4, i.e., now it has no hole. We assume that the deflexion vanishes on the convex portions of $\partial\Omega$ highlighted with thicker lines, and prescribe zero normal forces on its concave portions. Here again we take $f \equiv 1$. Meshes of a quarter domain indexed by an integer M are generated in a way quite similar to Test-problem 4.1.1, but now each one of them contains $2M^2$ triangles, like in the case of the ellipse. We display in Table 6 the same kind of results as in Table 5. Here again both methods appear to be equivalent in the sense of such maximum values, but now they seem to converge only linearly to the maximum value of the exact solution. In this case this is rather natural, if we consider solution's presumably low regularity, owing to the abrupt change of boundary conditions.

Table 6 – Solutions' maximum absolute values at element centroids for Test-problem 4.1.2

M →	8	16	32	64	128
h →	0.31250000	0.15625000	0.07812500	0.03906250	0.01953125
Hermite variant of RT_0 ($U_h=V_h$)	1.3240208	1.2859156	1.2608626	1.2460173	1.2377800
Modified Hermite variant of RT_0	1.3244286	1.2863349	1.2610147	1.2460619	1.2377921

Remark : A partial conclusion of Test-problems 4.1.1 and 4.1.2 is that our technique to handle with Hermite finite elements prescribed normal derivatives on curved boundaries is not so interesting in the case of low order methods. Nevertheless in the next sub-section we address a situation which somehow contradicts such a view. ∎

4.2 A tangential-displacement free finite-element model for plates

In the framework of the theory of plates and shells practitioners must take into consideration situations where the body's edge undergoes no displacement in the direction tangent to it. For example, this happens in the study of bucking of plates subjected to plane displacements (see e.g. [4]). Of course it is not our intention to address here complex problems of the kind, but just study a numerical method particularly suitable to simulate small plane deformations of curved plates whose edge displacement is normal to it. Like in Sub-section 4.1 the method is a Hermite variant of the lowest order Raviart-Thomas mixed finite element RT_0, though in vector version, since the unknown here is a two-dimensional displacement field. As a matter of fact this Hermite method was first developed in [9] to solve Maxwell's equations of electro-magnetism, in which case the electric field also satisfies zero tangential-component boundary conditions. Except for physical constants, the stationary counterpart of Maxwell's equations studied in [9] is very similar to the system that we are going to address here. For this reason the author refers to this work for more details on the method to be experimented in this sub-section, in the simulation of some simple curved plate deformation test-problems.

Here we consider a particular form of the homogeneous isotropic linear elasticity system in a two-dimensional domain Ω occupied by plate's mid-plane, satisfied by the displacement field $\mathbf{u} = (u_x, u_y)$. More particularly we assume that the plane force $\mathbf{g} = (g_x, g_y)$ acting on the edge of the plate is normal to it, and thus we may write $\mathbf{g} = g \mathbf{n}$, where g is a scalar function and $\mathbf{n}$ is the unit outer normal vector to the boundary $\partial\Omega$ of Ω. Then μ and λ being the Lamé constants of the material of the plate, under the conjugate action of body forces $\mathbf{f} = (f_x, f_y)$ the equations to solve are $- \mu \Delta\mathbf{u} - (\mu+\lambda)grad\,[div\,\mathbf{u}] = \mathbf{f}$ in Ω, with the boundary conditions $\mathbf{u} \times \mathbf{n} = \mathbf{0}$ and $(2\mu+\lambda)\,div\,\boldsymbol{u} = g$ on $\partial\Omega$.

Recalling the finite element set of functions V_h defined in the previous section, we define a space $\mathbf{W}_h$ consisting of fields $\mathbf{v}$ whose components belong to V_h, in the case where no zero values of normal derivatives along edges contained in $\partial\Omega_h$ have to be enforced. Then we define two subsets $\mathbf{V}_h$ and $\mathbf{V}_{h, g}$ of $\mathbf{W}_h$ as follows. Denoting by $\mathbf{n}_h$ the unit outer normal vector along $\partial\Omega_h$, $\mathbf{V}_h$ consists of fields $\mathbf{v}$ such that (the constant) $\partial(\mathbf{v} \cdot \mathbf{n}_h)/\partial n_h = 0$ along all the edges e_T of $\partial\Omega_h$ (cf. Figure 1). $\mathbf{V}_{h, g}$ in turn consists of fields $\mathbf{w}_h$ whose value $\partial(\mathbf{w}_h \cdot \mathbf{n}_h)/\partial n_h$ along any edge e_T of $\partial\Omega_h$ equals $g(P_T)/(2\mu+\lambda)$, where, naturally enough, P_T is the nearest intersection with $\partial\Omega$ of the perpendicular to e_T passing through the mid-point M_T of this edge. Differently from the case of the previous sub-section, here P_T will be the nearest intersection with $\partial\Omega$ of the perpendicular to e_T passing through the mid-point M_T of this edge. Then, quite analogously to the previous sub-section, a finite-element approximation $\mathbf{u}_h$ of $\mathbf{u}$ in the set $\mathbf{V}_{h, g}$, is a (presumably unique) solution to the following problem :

$$-\sum\nolimits_{T\,\text{in}\,\mathbf{T}_h} \Big[\int_T \{\mu(\Delta\mathbf{u}_h \cdot \mathbf{v}+grad\,\mathbf{u}_h \cdot grad\,\mathbf{v}+\mathbf{u}_h \cdot \Delta\mathbf{v})+(\mu+\lambda)grad\,div\,\mathbf{u}_h \cdot \mathbf{v})\}d\mathrm{x} \Big] = \int_{\Omega_h}\mathbf{f} \cdot \mathbf{v}\,d\mathrm{x} \text{ for all } \mathbf{v} \text{ in } \mathbf{V}_h \text{ (4)}$$

Notice that, similarly to (3), problem (4) mimics a mixed formulation of our problem, in which the boundary condition $\mathbf{u} \times \mathbf{n} = \mathbf{0}$ is handled as a do-nothing (Neumann) boundary condition, and $(2\mu+\lambda)\,div\,\boldsymbol{u} = g$ on $\partial\Omega$ is viewed as a Dirichlet boundary condition. Indeed the former condition will be automatically enforced (in a weak sense), since we do not require anything from $\partial(\mathbf{v} \times \mathbf{n}_h)/\partial n_h$ along $\partial\Omega_h$. It is also important to stress that in problem (4) the latter boundary conditions are shifted from the true boundary $\partial\Omega$ to the boundary $\partial\Omega_h$ of the polygon approximating the curved domain Ω. We will next show that in the case of the problem under study such an approach is disastrous.

We recall that in this work we want to focus on issues related to conditions prescribed on curved boundaries. That is why we will solve a modified problem for which on the one hand $\mathbf{f} \equiv \mathbf{0}$, like in

most practical situations, while on the other hand the divergence of **u** is known everywhere in Ω beforehand, namely, *div* **u** $= f$ *in* Ω, with $f := g / (2\mu+\lambda)$ on $\partial\Omega$. Thus we will actually solve:

$$ -\sum_{T \text{ in } \mathbf{T}_h} \left[\int_T \mu \left(\Delta\mathbf{u}_h \cdot \mathbf{v} + grad\ \mathbf{u}_h \cdot grad\ \mathbf{v} + \mathbf{u}_h \cdot \Delta\mathbf{v} \right) dx \right] = \int_{\Omega_h} \mathbf{f} \cdot \mathbf{v}\ dx \quad \text{for all } \mathbf{v} \text{ in } \mathbf{V}_h, \qquad (5) $$

where **f** $= (2\mu+\lambda)$ *grad f*. It is noteworthy that (5) is placed in the same functional setting as the one in [9] for Maxwell's equations. Hence we can claim second order convergence of $\mathbf{u}_h$ to **u** in the mean-square norm, in case Ω is a rectangle, for example. However as seen below, this will no longer be the case of a curved Ω.

In a first test-problem Ω is a disk with radius equal to 0.5 in a certain system of units, in which *g* is a constant equal to one as well, at every point of $\partial\Omega$. Assuming a Poisson ratio equal to 1/4, we have $\lambda = \mu$ and therefore the exact solution is given by $\mathbf{u}(x,y) = (\ x\ ;\ y\ )\ [x^2 + y^2]^{1/2} / 3\mu$. Computing with meshes for the whole disk, derived from those of Section 3.1 for the quarter disk using symmetry with respect to the coordinate axes, we obtain the results displayed in Table 7. Here *M* is the number of subdivisions of a diameter instead of a radius.

Table 7 – Errors for a circular plate problem solved by (5) shifting boundary conditions on *div* **u** to $\partial\Omega_h$

$M \rightarrow$	4	8	16	32	64
$h \rightarrow$	0.250000	0.125000	0.062500	0.031250	0.015625
Mean-square norm of $\mathbf{u}_h - \mathbf{u}$	0.51236×10^{-1}	0.51959×10^{-1}	0.52155×10^{-1}	0.52205×10^{-1}	0.52217×10^{-1}
Mean-square norm of *grad* ($\mathbf{u}_h - \mathbf{u}$)	0.21710×10^{0}	0.21114×10^{0}	0.20947×10^{0}	0.20903×10^{0}	0.20892×10^{0}
Max | $\mathbf{u}_h - \mathbf{u}$ | at element centroids	0.67396×10^{-1}	0.75965×10^{-1}	0.79763×10^{-1}	0.81574×10^{-1}	0.82464×10^{-1}

Table 7 shows that no convergence to problem's exact solution occurs if the boundary conditions on the normal component of the normal force are shifted from the true boundary to the boundary of the polygon Ω_h . It even seems that convergence to the solution of another problem is taking place.

In view of these unacceptable results, akin to Sub-section 4.1.1, we next endeavor to modify scheme (5), in order to recover method's orders that hold in case Ω is a polygon. Here our boundary condition interpolation technique will be accomplished by requiring that the divergence of $\mathbf{u}_h$ **at the above defined point** P_T located on $\partial\Omega$ next to a mesh triangle *T* having an edge e_T contained in $\partial\Omega_h$ (cf. Figure 1) equals $g(P_T)$. Notice that, akin to the previous sub-section, we could as well choose another boundary point at which the Dirichlet boundary condition on the divergence is to be enforced. However the above choice is particularly handy, since in the case of a disk the normal to $\partial\Omega$ at P_T is aligned with the normal to e_T .

Now, we make use of the expression of the divergence operator on the boundary of Ω in local curvilinear coordinates, namely, *div* **v** $= \partial(\mathbf{v} \cdot \mathbf{n})/\partial n + \partial(\mathbf{v} \cdot \mathbf{t})/\partial t + (\mathbf{v} \cdot \mathbf{n}) / R$, where **t** is the unit tangent vector along $\partial\Omega$, $\partial(\cdot)/\partial t$ denotes the partial derivative along **t**, and *R* is the local curvature radius of $\partial\Omega$. Noticing that we expect the tangential component of $\mathbf{u}_h$ along $\partial\Omega$ to vanish, it seems reasonable to require that $[\partial(\mathbf{u}_h \cdot \mathbf{n})/\partial n + (\mathbf{u}_h \cdot \mathbf{n}) / R](P_T) = g(P_T)$. Actually the values of $\partial(\mathbf{u}_h \cdot \mathbf{n})/\partial n$ and $\mathbf{u}_h \cdot \mathbf{n}$ at P_T are taken from the expression of $\mathbf{u}_h$ in *T,* even though extended outside this triangle. Of course in the present case $R = 0.5$ everywhere.

In Table 8 we supply the same kind of errors for our modified approach as in Table 7. One can clearly observe solution's second order convergence in the mean-square norm, while optimal first order convergence of the solution gradient – hence of the deformation –, seems to hold in the same norm.

Table 8 – Errors for model (5) assigning divergence values on the true boundary of a circular plate

$M \rightarrow$	4	8	16	32	64
$h \rightarrow$	0.250000	0.125000	0.062500	0.031250	0.015625
Mean-square norm of $\mathbf{u}_h - \mathbf{u}$	0.19125×10^{-2}	0.49514×10^{-3}	0.12505×10^{-3}	0.31358×10^{-4}	0.78381×10^{-5}
Mean-square norm of $grad\,(\mathbf{u}_h - \mathbf{u})$	0.31326×10^{-1}	0.16059×10^{-1}	0.80808×10^{-2}	0.40471×10^{-2}	0.20247×10^{-2}
Max $\mid \mathbf{u}_h - \mathbf{u} \mid$ at element centroids	0.26213×10^{-2}	0.70591×10^{-3}	0.18255×10^{-3}	0.46882×10^{-4}	0.11948×10^{-4}

Since one might object that circular plates are too simple and particular, to conclude this sub-section we assess the above technique to treat zero edge tangential displacements for a different geometry. More specifically we apply the numerical model (5) assorted with our Dirichlet boundary condition interpolation technique, to the following toy-problem in an ellipse with semi-axes equal to c and 1. We take $\mu = \lambda = 1$, $\mathbf{f} = ([6 + 2c^2]x\,;\,[2 + 6c^2]c^2 y)$ and $g = -3[(3 + c^2)x^2 + (1 + 3c^2)c^2 y^2]$. The exact solution is $\mathbf{u} = -([x^2 + c^2 y^2]x\,;\,[x^2 + c^2 y^2]c^2 y)$. We construct meshes for the whole ellipse in the same way as for the circular plate, by adjusting just the radial coordinate, in order to take into account the ellipse's equation in polar coordinates instead of a constant one. For convenience we redefine $h = 2c/M$, taking $c = 0.5$.

We give in Table 9 the same kind of errors as in Table 8. These results confirm that for arbitrary smooth curved domains, practically the same behavior as in the circular case can be expected, as long as the modification advocated in this subsection is implemented, to treat (Dirichlet) boundary conditions on the normal component of a boundary traction field.

Table 9 – Errors for a toy-problem (5) in an ellipse assigning values of *div* $\mathbf{u}_h$ on the true boundary

$M \rightarrow$	4	8	16	32	64
$h \rightarrow$	0.250000	0.125000	0.062500	0.031250	0.015625
Mean-square norm of $\mathbf{u}_h - \mathbf{u}$	0.17029×10^{-1}	0.48793×10^{-2}	0.12637×10^{-2}	0.31846×10^{-3}	0.79764×10^{-4}
Mean-square norm of $grad\,(\mathbf{u}_h - \mathbf{u})$	0.14110×10^{0}	0.75943×10^{-2}	0.38734×10^{-2}	0.19464×10^{-1}	0.97442×10^{-2}
Max $\mid \mathbf{u}_h - \mathbf{u} \mid$ at element centroids	0.22458×10^{-1}	0.71142×10^{-2}	0.20015×10^{-2}	0.53302×10^{-3}	0.13804×10^{-3}

Remark : In contrast to the approach employed in Section 3 to solve the curved membrane problem with quadratic finite elements, in the case of our Hermite variant of the mixed method RT_0 it is not necessary to recalculate the basis corresponding to the modification of the sets V_h and $\mathbf{V}_{h,\,g}$, advocated in this section. This is due to the particularly simple representation of the unknown function or field at element level. Indeed, the function or field itself have no boundary degree of freedom to adjust, while its normal derivative within a boundary triangle T varies linearly in the directions orthogonal to edge e_T and is constant along any segment parallel to it. Hence recalculation of such bases to fit an edge parallel to e_T tangent to $\partial\Omega$ will necessarily result in the expressions already determined for $V_{h,}$. ∎

5 Conclusion and final comments

Globally, on the basis of the numerical experiments reported in this work for various problems of Continuum Mechanics posed in curved bounded domains, we can assert that our new method to handle Dirichlet boundary conditions with higher order finite element methods, provides a simple and reliable tool to overcome technical difficulties brought about by complicated situations and/or interpolations.

This technique was illustrated here in the two-dimensional case, for classical Lagrange finite elements, and for a Hermite analog introduced in [8] and [9] in scalar and vector versions respectively, of the method RT_0 – the Raviart-Thomas mixed finite element method of the lowest order –, for equations with normal derivative or flux boundary conditions. In the case of Lagrange finite elements a theoretical justification of our approach's optimality was given in [7]. In a forthcoming paper we intend to extend this study to the Hermite variant of the RT_0 method, and eventually to the whole Raviart-Thomas family of mixed methods (cf. [6]).

Incidentally we observe that in case Neumann boundary conditions are prescribed, optimality of Lagrange finite elements can only be recovered if the variational problem's right hand side is modified. Referring to Figure 1 this modification consists of shifting boundary integrals for elements in $\mathbf{S}_h$ to the curved boundary portion of an element sufficiently close to the one of the corresponding curved element T'. However this is an issue that has nothing to do with our method, for it is basically aimed at resolving those related to the prescription of degrees of freedom, in the case of Dirichlet boundary conditions.

As the reader has certainly noticed, our method leads to well-posed problems, though with a non symmetric matrix. Moreover in order to compute the element matrix and right hand side vector for a boundary element in $\mathbf{S}_h$, in principle it is necessary to determine the inverse of an $n \times n$ matrix, where n is the number of local degrees of freedom of the method under use. However this extra effort should by no means be a problem at the current state-of-the art of Scientific Computing, as compared to the situation by the time isoparametric finite elements were introduced.

Finally the author would like to stress that his technique applies without any particular difficulty, to the extremely important three-dimensional case. An ongoing work of his is aimed at supporting this assertion.

References

[1] F. Bertrand, S. Münzenmaier and G. Starke, First-order system least-squares on curved boundaries: higher-order Raviart-Thomas elements, *SIAM J. Numerical Analysis*, 52-6 (2014), 3165-3180.

[2] S.C. Brenner and L.R.Scott, The Mathematical Theory of Finite Element Methods, Texts in Applied Mathematics 15, Springer, 2008.

[3] P.G. Ciarlet, The Finite Element Method for Elliptic Problems, North Holland, Amsterdam, 1978.

[4] R.M. Jones, Buckling of Bars, Plates, and Shells, Bull Ridge Corp., 2006.

[5] J. Nitsche, On Dirichlet problems using subspaces with nearly zero boundary conditions. The Mathematical Foundations of the Finite Element Method with Applications to Partial Differential Equations, A.K. Aziz ed., Academic Press, 1972.

[6] P.-A. Raviart and J.-M. Thomas, Mixed Finite Element Methods for Second Order Elliptic Problems, Lecture Notes in Mathematics, Springer Verlag, 606: 292--315, 1977.

[7] V. Ruas, Optimal simplex finite-element approximations of arbitrary order in curved domains circumventing the isoparametric technique, *arXiv* :1701.00663, 2017.

[8] V. Ruas, Hermite finite elements for second order boundary value problems with sharp gradient discontinuities, *Journal of Computational and Applied Mathematics*, 246 (2013), 234-242.

[9] V. Ruas and M.A. Silva Ramos, A Hermite finite element for Maxwell's equations, AIP Proceedings of ICNAAM, T. Simos ed., Rhodes, Greece, 2016.

[10] L R. Scott, Finite Element Techniques for Curved Boundaries. PhD thesis, MIT, 1973.

[11] O.C. Zienkiewicz, The Finite Element Method in Engineering Science, McGraw-Hill, 1971.